


A climatology of weather-driven anomalies in European photovoltaic and wind power production

Linh Ho-Tran ^{1,2}✉ & Stephanie Fiedler^{1,2,3}

Weather causes extremes in photovoltaic and wind power production. Here we present a comprehensive climatology of anomalies in photovoltaic and wind power production associated with weather patterns in Europe considering the 2019 and potential 2050 installations, and hourly to ten-day events. To that end, we performed kilometer-scale numerical simulations of hourly power production for 23 years and paired the output with a weather classification which allows a detailed assessment of weather-driven spatio-temporal production anomalies. Our results highlight the dependency of low-power production events on the installed capacities and the event duration. South-shifted Westerlies (Anticyclonic South-Easterlies) are associated with the lowest hourly (ten-day) extremes for the 2050 (both) installations. Regional power production anomalies can differ from the ones in the European mean. Our findings suggest that weather patterns can serve as indicators for expected photovoltaic and wind power production anomalies and may be useful for early warnings in the energy sector.

¹Institute of Geophysics and Meteorology, University of Cologne, Cologne, Germany. ²GEOMAR Helmholtz Centre for Ocean Research Kiel, Kiel, Germany. ³Faculty of Mathematics and Natural Sciences, Christian-Albrechts-University of Kiel, Kiel, Germany. ✉email: Lho@geomar.de

European countries are collectively facing pressing challenges in securing electricity supply with an increasing share of renewable energy. One of the challenges is the dependency of wind and solar power on the weather, which is especially critical when one or both power productions are anomalously low due to adverse weather conditions. The weather dependency is expected to increase in the future as the European Union plans to produce more energy from renewable sources to become climate-neutral by 2050¹. Therefore, it is important to study which weather conditions are related to extreme anomalies in wind and solar power production, and how their anomalies are spatially distributed across Europe. Such knowledge can help the electricity system operators to prepare counter-measures, e.g., with an adequate national and cross-border transmission grid for electricity^{2,3} that could make use of natural balancing effects arising from regional weather differences⁴.

Accounting for the weather impacts in energy system analyses has been attracting research contributions from the energy and meteorological perspectives. A few studies have addressed how synoptic weather conditions influence resources for wind and solar power production, but for past power installations or for a certain region only or limited to 1-day anomalies^{5–10}. The definition and classification of synoptic weather conditions varied across studies and often gave insights with some limitations as follows. According to a composite analysis based on sea level pressure, high-pressure systems over central Europe are associated with 1-day low power production¹¹. Others used up to seven weather regimes, i.e., synoptic weather systems that vary on weekly timescales^{7,12}, and show that European blocking high-pressure systems are associated with negative anomalies in renewable power production^{7,9}. Classifications of weather closer to 30 categories represent more details for the day-to-day variability and regional differences in the weather¹³. Higher spatial resolution and the analogy to meteorological charts make using weather patterns more applicable for electricity system operators. To the best of our knowledge, there is no study addressing this need with the necessary spatio-temporal detail using projected future installed capacities for photovoltaic (PV) and wind power production paired with a systematic assessment of power anomalies across Europe that have durations of one to up to ten days. Our study aims to contribute to filling this knowledge gap. The different duration of production anomalies is relevant since the security of supply depends not only on the daily power production but also on the load of storage capacities that are influenced by the sequence of weather over several days⁹, e.g., investigated with an energy-system model for Germany¹⁴.

This study presents to the best of our knowledge the first comprehensive kilometer-scale assessment of the effects of weather patterns on the spatiotemporal anomalies in PV and wind power production of different lengths for present and projected future installations in Europe. To that end, we have developed the Renewable Energy Model (REM) that simulates PV and wind power production using hourly meteorological data for 23 years (1995–2017) with an effective horizontal resolution of 6 km. We implemented gridded scenario data for installed capacities of PV and wind power for 2050¹⁵, which was not done for past assessments for power production anomalies associated with different weather patterns^{6,7,10}. Using gridded data is, however, important for assessments of weather and climate influences on the energy system¹⁶. Specifically, a kilometer-scale hourly resolution is important for the link between weather and power production because such an approach is substantially closer to the typical scales for energy applications, which cannot be accomplished with the often country-aggregated assessments in past studies^{4,6,7,10}. To investigate how power production anomalies are associated with different weather patterns and how the

dependency changes with the projected future power installations, we perform and inter-compare several REM simulations. Most of our results are based on the following two REM simulations (see Methods for details):

- Scenario-2050 is the REM simulation with the CLIMIX¹⁵ scenario for PV and wind power installations for 2050. This scenario reflects a substantial increase in the share of PV power production compared to 2019¹⁷. REM yields a share of the PV power production to the PV plus wind power production of 46%, which falls within the range of the suggested optimal share of 45–57% to minimize the spatial variability by changing weather and seasonal variability in power production^{4,18}.
- Scale-2019 is the REM simulation where we scale the installed capacities from scenario-2050 with constant values to match with the Europe-aggregated installed capacity of PV and wind power in 2019¹⁷. The ratio of PV to PV plus wind power production is 24%, which is about half of that in 2050 and similar to other calculations for present-day Western Europe¹¹. Our approach retains the spatial distribution of 2050 and decreases the magnitude of installations by multiplying scaling factors. This choice was made due to the lack of a gridded dataset for present-day installed capacity with a 6 km resolution. The results proved useful for our assessment and successfully reproduced past results for Germany with present-day capacities⁶.

The output of the REM simulations is paired with an established classification of 29 synoptic weather patterns from the German Weather Service¹⁹. This daily weather classification is based on an automated identification algorithm of patterns in charts of the mean sea-level pressure and the 500 hPa geopotential height. An expert control ensures the quality of the automatically identified weather pattern¹⁹. The classification data allows us to examine the weather dependency of future installed capacities for wind and PV power associated with different weather patterns for Europe using quality-controlled weather patterns of the past. Using synoptic weather patterns is desirable since this method is well established and routinely diagnosed as weather service. Our results point to specific weather patterns for anomalously low PV plus wind power production in Europe depending on the installation and event duration. For instance, the lowest hourly PV plus wind power productions are simulated during weather patterns with very regionally low wind speeds for the present-day installation while weather patterns for dark doldrums coincide with the lowest wind plus PV production for the 2050 installation, consistent with the higher share of PV power in 2050. Ten-day events with the lowest wind plus PV power production are associated with prolonged anticyclonic weather patterns for both installations. As such the weather pattern could give a first indication of whether power production anomalies are to be expected with the coming weather for a future PV and wind power installation—an aspect of growing importance when we move from primarily fossil fuel-based power technologies to an increasing share of renewable sources for climate change mitigation.

Results

European mean power production. We find substantial differences in the European PV plus wind power production (hereafter total production) depending on the weather pattern. Wind power production has a prevalent impact on the total output independent of the installed capacities with onshore and offshore installations typically having equal contributions. This can be

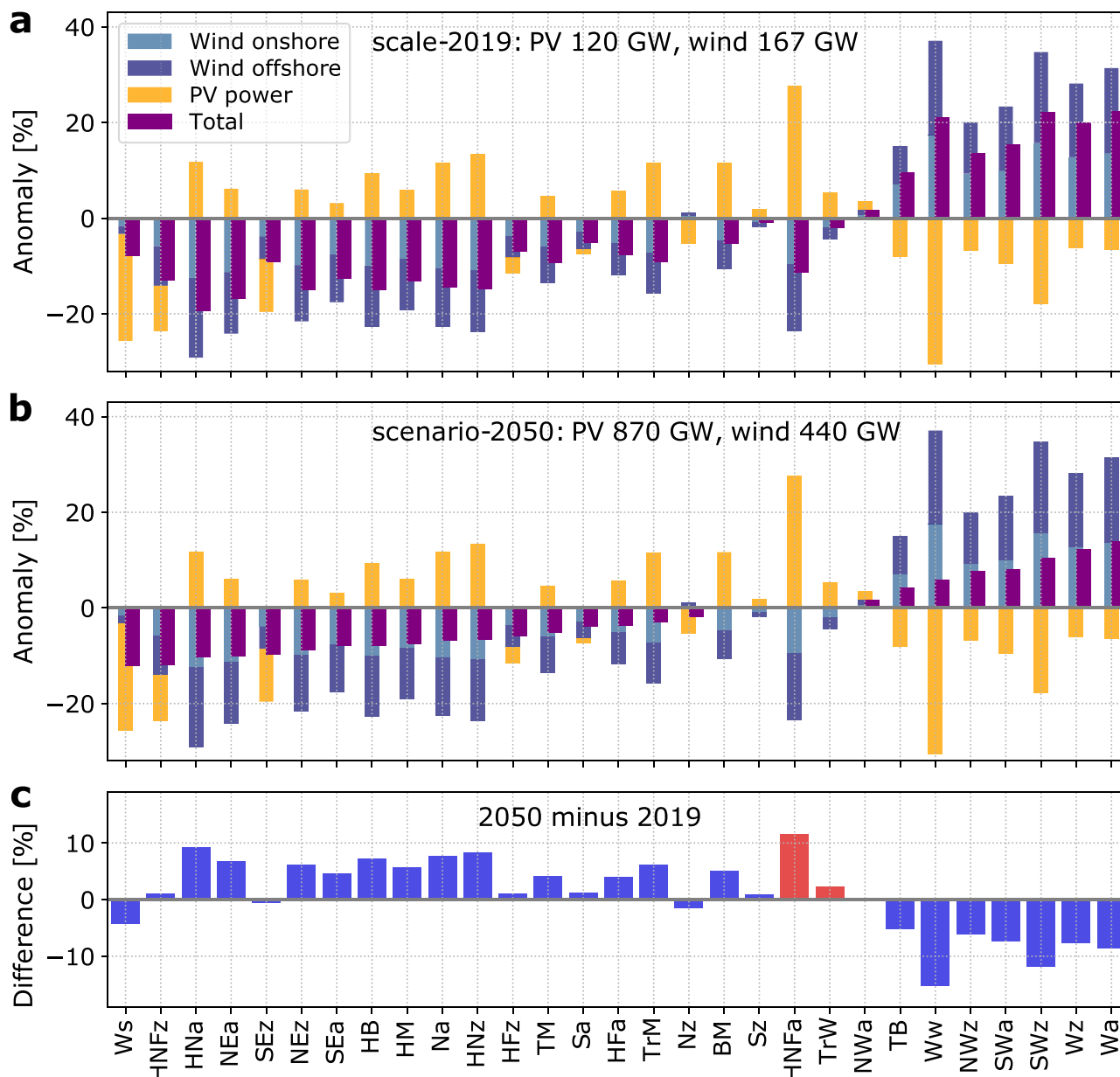


Fig. 1 Anomalies in power production associated with weather patterns in Europe. Anomalies in photovoltaic (PV), offshore, and onshore wind power production (stacked) as well as PV plus wind power (total) associated with weather patterns as simulated by (a). scale-2019 and (b). scenario-2050. Differences in the anomalies of total production associated with different installed capacities are shown as (c). scenario-2050 minus scale-2019. Red bars in (c). mark weather patterns where the sign of the anomaly depends on the installed capacities. Results in (a-c) are sorted by increasing total production from left to right based on scenario-2050 in (b).

seen from the similar behavior of anomalies in wind power production and total power production across weather patterns (Fig. 1a, b). Seven out of eight weather patterns with westerly winds, indicated by the letter W in the name, have a composite European total production higher than the climatological mean for 1995–2017 (Fig. 1a, b). The only exception is the South-Shifted Westerly pattern (Ws), which has the lowest European total production and will be discussed in detail later. Positive anomalies in PV power production have mostly northerly and northeasterly winds (with letters N and NE). The last character in their names refers to their cyclonic or anti-cyclonic characteristic, i.e., a low-pressure system with cyclonic flow indicated by the letter z (zyklonal in German) and a high-pressure system with anticyclonic flow marked with the letter a¹⁹. Nine out of thirteen weather patterns associated with anomalously high PV power

production have an anticyclonic characteristic, typically associated with anomalously high irradiance due to lower cloud cover (Fig. 1a, b). Values of power production anomalies associated with the weather patterns along with their names can be found in Supplementary Table S1.

Our results for scale-2019 installed capacities are consistent with earlier findings for Germany⁶. We see that the pattern of High pressure over Central Europe (HM) is associated with the lowest total production for Germany (see Supplementary Fig. S1). In the European mean, however, HM is associated with the 7th lowest total power production and is, therefore, less extreme when we assess a much larger area. From the European perspective, extremes in power production in single countries can theoretically be balanced with production in other countries in most cases⁴, and this is also true for production shortages in the German energy system¹⁴.

future climate change, with an overview based on EURO-CORDEX experiments²¹. The impact of climate change on PV power production is not a focus of our study.

Natural balancing effects between PV and wind power production reduce the magnitude of anomalies in total power production, independent of the weather pattern and the installed capacities. This is seen by the consistently smaller anomaly in the total power production compared to either the anomaly in PV or wind power production (Fig. 1a, b). The range in anomalies across all weather patterns, i.e., the highest anomaly minus the lowest anomaly, in the total production in scenario-2050 (26%) is reduced by one-third compared to that of scale-2019 (42%). This reduction implies that a high share of PV power in scenario-2050 improves the potential for balancing effects in meteorological variability for the European energy system, previously suggested by other studies^{4,18}.

We test to what extent an even higher share of PV power installations could contribute to the balancing effect. To that end, we perform a sensitivity experiment with REM, where PV power installed capacity is five times larger than that of wind power, equivalent to a PV power contribution of 69% to the total production. This contribution of PV power is higher than the optimal share 45–57% of PV to PV plus wind power production that was estimated from weather and installations of the past^{4,18}. Increasing the installed capacities for PV power further reduces anomalies in total production associated with some of the weather patterns, e.g., HNa and HM have now near-average total production (Supplementary Fig. S3) in contrast to the below-average production of –10 and –8% in scenario-2050. There is, however, no large difference in the range of the total production anomalies with a slight increase by 3% compared to scenario-2050, consistent with the optimum being already reached for lower PV shares^{4,18}. This finding implies that there are benefits of an even higher share of PV power production during individual weather patterns, but it does not reduce the overall natural variability in power production for all weather patterns.

Seasonal differences. We assess the differences in anomalies in the total power production associated with different weather patterns for the winter and summer half-year (Fig. 3 and details for PV and wind power in Supplementary Fig. S4). We use here the same half-year definition as for the weather patterns¹⁹, i.e., 16 October to 15 April for winter, and 16 April to 15 October for summer.

The results highlight that weather patterns associated with above-average wind power production are good indicators for above-average total production for the 2019 and 2050 installations (group High wind in Fig. 3a, b). The group High wind dominates the weather during winter with an occurrence frequency of 60% (Fig. 3c). Looking at individual patterns in the group High wind suggests typically small seasonal differences in the associated total power production, compared to the group High PV. The seasonal differences are larger and not systematic across the patterns in the group High wind for scale-2019. For scenario-2050, however, most weather patterns in the same group High wind are associated with more production in the winter, except Low Pressure over the British Isles (TB, Fig. 3a, b). Result for smaller sub-regions of Europe can be different, e.g., SWz, Wz, and NWz in the group High wind for European power production show over region A the characteristics of a dark doldrum (see Supplementary Fig. S2).

Most weather patterns in group High PV typically have higher mean total production in summer than in winter (Fig. 3a, b), consistent with the naturally higher irradiance and lower wind power production during summer for these patterns (Fig. 2). This

is true for both installed capacities. Weather patterns from group High PV dominate the weather in summer with an occurrence frequency of 58%.

Interestingly, the lowest winter total production falls into the group High PV for both installations, namely Icelandic High with Ridge Central Europe (HNa). We find an anomaly of –24% in the total winter power production for HNa in scale-2019 with simultaneously below-average PV and wind power production (see Supplementary Fig. S4). During winter, HNa therefore has a characteristic behavior of a pattern in the dark doldrum explained by the lower irradiance and the potential fog formation during high-pressure influence in winter. This is different in summer when high pressure often leads to cloud-free skies allowing more irradiance consistent with the anomalously high PV power production for HNa in the annual mean (Fig. 1a, b). This finding points to a seasonal dependency of the dark doldrums characteristics.

In the group Dark doldrums, SEz has the largest seasonal differences. In the summer, it can lose the characteristic behavior of a dark doldrum due to near-average total production for both installations (Fig. 3a, b), primarily driven by above-average wind power production in the summer (Supplementary Fig. S4). On the other hand, patterns HNFz and Ws consistently show characteristics of a dark doldrum, with both PV and wind power production simultaneously below the average in both seasons and for both installations (Supplementary Fig. S4). For this reason, they have very small seasonal differences for total production, especially in the future installation. They produce the lowest all-year total production in scenario-2050 (Fig. 1b), although they are not associated with seasonal extremes, having the 4th and 11th lowest total production in the winter, respectively (Fig. 3b).

Spatial differences. We assess the spatial distribution of the most extreme anomalies in the mean all-year power production (Fig. 4). A complete pictorial atlas of spatial power anomalies associated with 29 weather patterns is given in Supplementary Fig. S5 along with statistical information (see Supplementary Table S1). We discuss here the patterns (1) HNa and Ws with the lowest total production in scale-2019 and scenario-2050, respectively, (2) Wa with the highest total production for both installations and (3) HNFa for the contrasting extremes in individual energy sources and the sensitivity to the installed capacities (Fig. 1b, c).

The pattern Icelandic High, Ridge Central Europe (HNa) (Fig. 4a–e) belongs to the group High PV with positive regional anomalies in PV power production and the lowest wind power production in the European mean (Fig. 1a). The ridge over Central Europe is associated with higher than average PV power production in Germany and Poland in contrast to weak winds around the North Sea, explaining the anomalously low wind power production with slightly more pronounced production reductions in offshore wind power compared to onshore in Europe (Fig. 1). Away from the ridge, the Iberian Peninsula receives relatively little irradiance and slightly above-average wind speeds. The combination of low wind power production around the North Sea and low PV power production in the Iberian Peninsula leads to anomalously low total power production in the European mean for scale-2019. A higher share of PV power in scenario-2050 helps the positive anomaly in PV power production over parts of Central and Northern Europe to better balance negative anomalies in wind power production in some areas in Germany and France. This effect is strong enough to increase the total power production associated with HNa, such that it does not have the lowest total production in scenario-2050.

The South-Shifted Westerly (Ws) belongs to the group Dark doldrums with simultaneously below-average PV and wind power

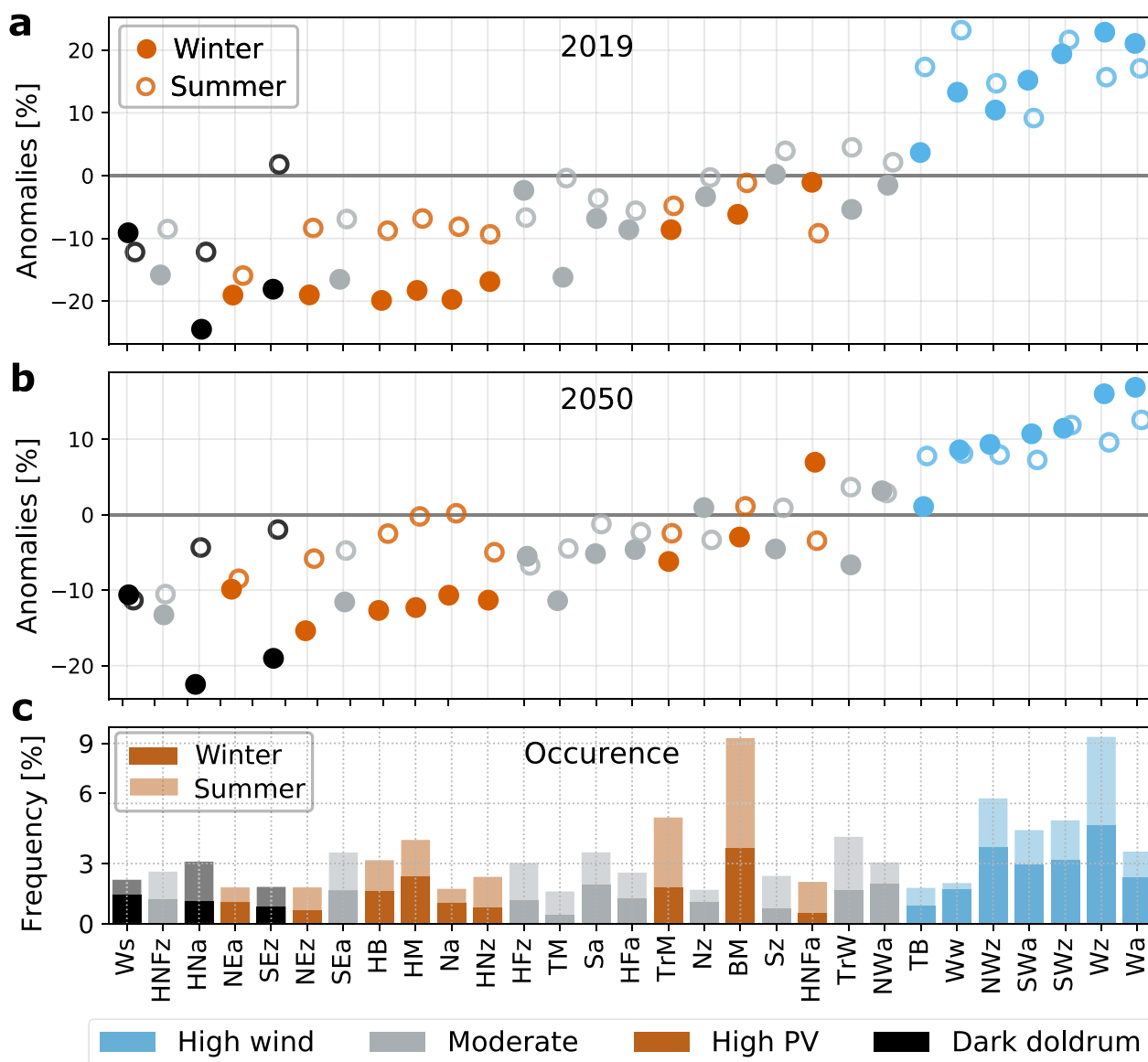


Fig. 3 Seasonal differences in power production anomalies. Total production anomalies in % as simulated by (a). scale-2019 and (b). scenario-2050, and (c). the seasonal frequency of the weather patterns (stacked), sorted by increasing magnitude of power production in scenario-2050 from left to right. The color-coded groups of weather patterns are marked as in Fig. 2. The seasons here are in half-year periods following the definition for the weather patterns¹⁹ with winter from mid-October to mid-April and summer from mid-April to mid-October. For the seasonal differences of PV and wind power production individually, refer to Supplementary Fig. S4.

production (Fig. 4f–j). PV power production is particularly low due to below-average irradiance across Europe along with a low-pressure system with the center over the North Sea. Wind speeds and hence the associated power production are anomalously high at the southern margin of the low-pressure system, i.e., across Central and Southern Europe. To the North, weak winds occur around the North Sea, the British Isles, and Scandinavia (Fig. 4a, d), leading to a slightly below-average wind power production for Ws for both installations (Fig. 1a, b). The combination of very low PV power production and the shortage of wind power production north of 51°N results in extremely low total power production across the northern regions for both installations (Fig. 4g, h). In scale-2019, south-western regions in Europe have slightly more areas with positive anomalies in total production, induced by a stronger influence of regionally high wind power production (Fig. 4g). The positive anomalies in these regions help

to better balance the negative anomalies in the northern regions, giving a total production for Europe with less negative anomaly than in scenario-2050 (Fig. 1a).

Anticyclonic Westerly (Wa) shows similar regional anomalies in total production for both installations that lead to the highest total production in the European mean. This result is mainly caused by the strong positive anomalies in wind power production in the North of Europe. The strong North-South pressure gradient between 49°N and 59°N causes strong westerly winds and therefore the anomalously high wind power production from the British Isles via the North Sea to the Baltic and the adjacent countries (Fig. 4k, o). The high wind power production explains the above-average total production for these regions which have large wind power plants. The pronounced regional impact of wind power gives Wa the highest total production in both seasons and for both installed capacities

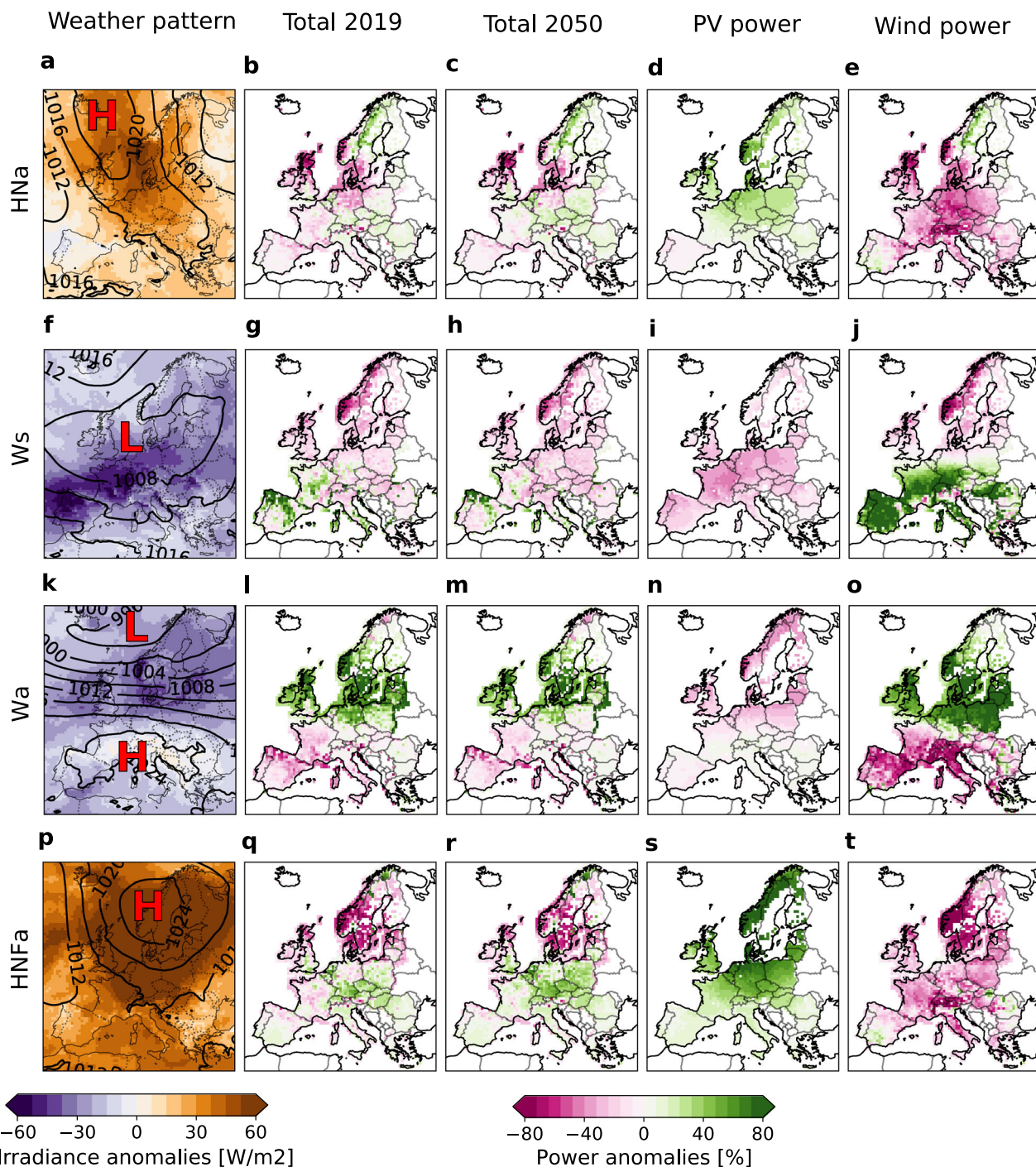


Fig. 4 Composite maps for production anomalies associated with four selected weather patterns. Spatial anomalies of power production associated with (a–e). HNa with the lowest total production simulated by scale-2019, (f–j). Ws with the lowest total production in scenario-2050, (k–o). Wa with the highest total production in both simulations, (p–t). HNFa with anomalies of opposite signs for PV and wind power production in both simulations. The first column shows the composite maps of mean sea level pressure (contours) with 4 hPa increments and shading for the irradiance anomalies. The other columns (left to right) show the spatial distribution of anomalies in total production from scale-2019 and from scenario-2050 installations, as well as the contributions from PV and wind power production anomalies. The full Atlas of production anomalies associated with the individual 29 weather patterns is shown in Supplementary Fig. S5.

(Figs. 3a, b, 1a, b, 4l, m), despite the below-average wind power production in Southern regions and below-average PV power production across most of Europe (Fig. 4n, o).

Weather patterns High Scandinavia-Iceland, Ridge Central Europe (HNFa) are characterized by a high-pressure system over Scandinavia causing anomalously high PV but anomalously low wind power production across all of Europe (Fig. 4p–t). Taken

together, we see a strong North-South difference in the sign and magnitude of anomalies in the total power production independent of the installation (Fig. 4q, r). The change in sign of the regional anomalies occurs around the latitudes 45–55°N. This behavior points to the usefulness of building North-South electricity transmission lines to balance naturally occurring regional extremes in power production due to the weather, even during days when the

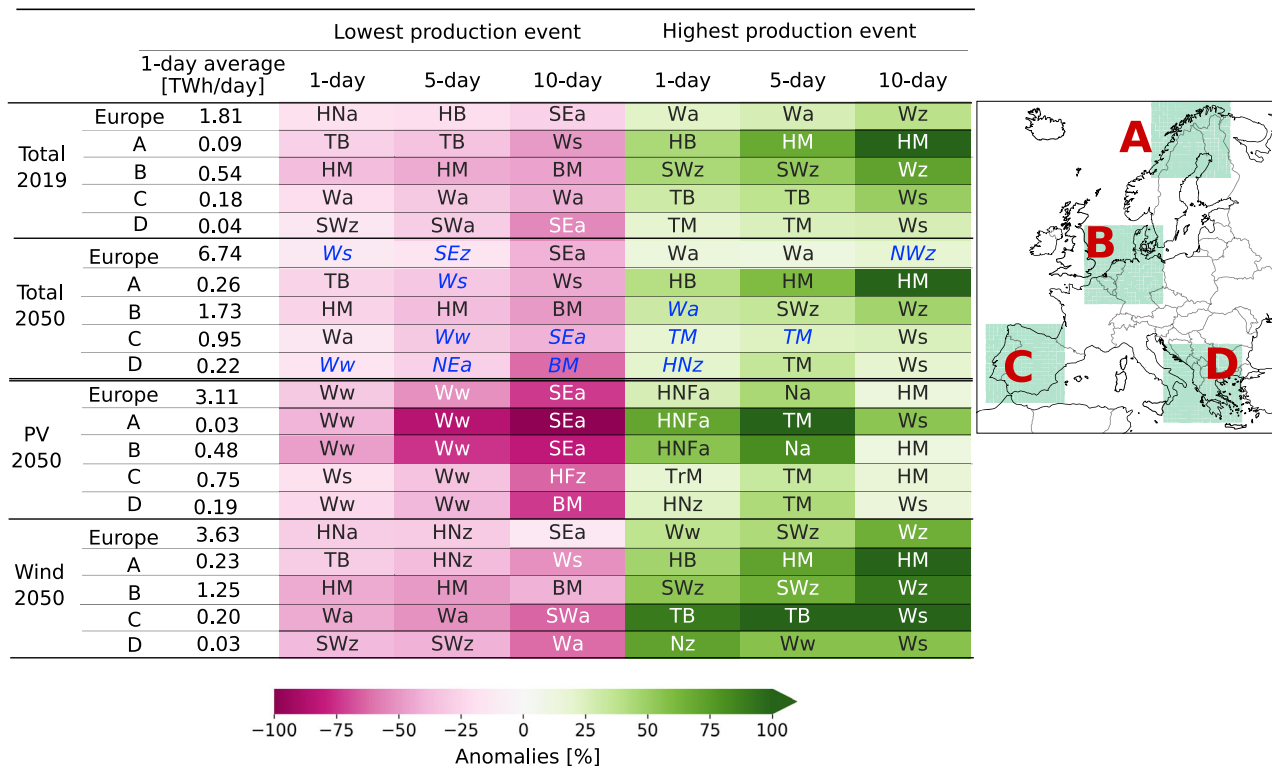


Fig. 5 Production extremes of different durations associated with weather patterns. Weather patterns associated with the lowest (magenta) and highest (green) production events that last at least one, five, and ten days for Europe and for the four regions marked on the map (A–D, see Methods). Blue marks where weather patterns leading to production extremes change from scenario-2050 to scale-2019. The results of sensitivity tests for intermediate event durations are shown in Supplementary Fig. S6.

weather has a similar influence on PV or wind power production for all of Europe.

Our results suggest that the balancing potentials strongly depend on the weather pattern and the installed capacity, such that the grid planning should not be based on coarse-grained data assessments. The regional differences such as in Wa specifically imply that aggregated power production for all of Europe or single countries is not always representative of all regions falling inside that area.

Duration differences. The impacts of an anomaly in power production are expected to be more severe the longer an event lasts. We conduct a quantitative assessment of the differences in power production associated with weather patterns prevailing for different numbers of days. To that end, we first identified events of consecutive days with the same weather pattern of at least one, five, and ten days, obtaining 8401, 443, and 19 events respectively during the period 1995–2017. We then identified from these events those that were associated with the lowest and highest daily power production, compared to the climatological daily mean shown in Fig. 5. We again use the same four regions (A–D) marked in Fig. 5) to demonstrate how the impacts of extreme production events, measured on the European scale, vary spatially across several regions.

For individual energy sources, weather patterns associated with 1-day and 5-day extremes in power production are often similar, but this is not true for 10-day events (Fig. 5). With increasing duration, the impacts of the associated anomalies in power production are expected to increase. This is indeed seen in our result by the increasing magnitude of the power production anomaly when we go from 1-day to 10-day events, e.g., the largest absolute magnitude of an anomaly in wind power for 1-day

events is 90% (region C), and for 10-day events is 137% (region A). However, this effect is not seen for the high production events for PV power. Specifically, the anomalies in the 10-day highest production events for PV power are often smaller than for the shorter durations. This is because all 19 10-day events occur during winter (mid October–mid April) and are typically associated with an anticyclonic weather pattern that would fall into the category of atmospheric blockings. This puts more weight on the darker winter time in their 10-day means and thus decreases the average production of PV power compared to shorter events.

The lowest 10-day total power production for Europe is seen for Anticyclonic South-Easterly (SEa) with mean anomalies of –27% and –41% for scale-2019 and scenario-2050, respectively. Interestingly, SEa exhibits the characteristic of a dark doldrum in the winter in this event (25/11–04/12/2014), with the 10-day lowest production for both PV and wind power (–73% and –13%), but the same pattern is not associated with extremes in 1- and 5-day power production means.

Balancing potentials for total power production exist for both installations, even for extreme power production events with a duration of several days. For instance, the pattern High over Central Europe (HM) is associated with the 1-day and 5-day lowest total power production in region B, consistent with an assessment for Germany⁶. In region A, however, the same weather pattern leads to the 5- and 10-day highest total power production, pointing to the balancing potential between Scandinavia and Germany as seen earlier in a comprehensive power system simulation for Germany¹⁴. Another example of such balancing potentials is seen in regions C and D which have the highest 10-day total production associated with Ws, opposite to region A which has the lowest 10-day total production associated with the same weather pattern. Pattern Cyclonic South-Westerly

(SWz) brings the lowest wind power production in 1- and 5-day events in region D, but brings the highest wind power production with the same durations for region B, agreed with a previous study⁷. It implies that an efficient European electricity grid covering large distances across several country borders would be beneficial to reduce regional impacts of weather-induced shortages in power production from wind and irradiance.

The result is robust for events shorter than 2 days, i.e., the associated weather patterns are identical for 1-day and 2-day events (Supplementary Fig. S6). For longer similar event durations, the weather patterns associated with anomalies in production are not always identical, especially for low-production extremes, but the patterns have similar characteristics. For example, SEz and Ws are associated with 5-day and 4-day low-production events in Europe and both belong to the group Dark doldrum. Also, NWz and NwA are associated with the highest 10-day and 8-day production events and have similar patterns in wind directions. The largest differences in the weather patterns are seen for prolonged events of 8 days and 10 days, which is consistent with comparably few cases of such extremes. Specifically, there is a total of 19 10-day events in the period 1995–2017, compared to 69 events with 8-day duration.

Discussion

We provide a comprehensive analysis of PV and wind power differences and extremes associated with different synoptic weather patterns for Europe with an high level of detail. Using an hourly weather dataset with 6 km horizontal resolution, and future power installations, we simulate PV and wind power production and pair the results with a routinely used weather pattern classification. We identify weather patterns associated with extreme power production averaged for Europe. These cause extreme anomalies in PV or wind power production individually, e.g., Maritime Westerly, Block Eastern Europe (Ww), and High Scandinavia-Iceland, Ridge Central Europe (HNFa), and in some rare cases simultaneously low PV and wind power production which we refer to as dark doldrum, e.g., South-Shifted Westerly (Ws). For present-day installed capacity, the pattern Icelandic High, Ridge Central Europe (HNa) with low wind speeds across most of Europe is associated with the lowest mean hourly total production (PV plus wind power). However, with a higher share of PV power in the projected future installed capacity of 2050, Ws produces the lowest hourly average of total production primarily due to anomalously low irradiance. Weather patterns that lead to extremely high wind power production, such as Wa, produce the highest hourly total production, independent of the installed capacities. Interestingly, the relative share of anomalies in onshore and offshore wind power production for Europe is typically similar independent of the weather patterns, although the estimate of the European mean wind power production for 2050 is by about a factor of four larger offshore (155.8 MW) than onshore (37.1 MW). It suggests expanding on and offshore capacities is equally useful from a large-scale perspective on weather-driven production anomalies.

Increasing the duration of weather patterns from one to ten days leads to changes in the patterns that lead to extremes in PV and wind power production. The patterns HNa and Ws are associated with the lowest 1-day total production in present and future installation, similar to results for hourly production. But the pattern Anticyclonic South-Easterly (SEa) stands out as the 10-day event with the lowest PV, wind, and total power production for both the present-day and future installations. Different weather patterns are associated with different durations for extreme power production events. This suggests that adequate monitoring is needed for potential warnings in different

timescales for weather-induced production shortages in a climate-neutral energy system. In particular, the longer events might be critical, as they increase the burden on the security of the electricity supply due to continuous demand for electricity and a declining load of storage. Prolonged SEa thus can be considered as a multivariate compound event, one of the four types of compound weather and climate events²². Optimized spatial distribution of renewable power plants alone cannot substantially reduce the maxima in the total residual demand²³, but storage capacities and transmission of electricity could balance residual loads arising from anomalously low production¹⁴.

Prolonged SEa is one example of weather patterns with a high-pressure system that prevails over several days, commonly known as atmospheric blocking. Blocking events are known challenges for power production in energy systems of Europe^{7,24} and on other continents^{25,26}. The benefit of using the detailed weather pattern classification in our study compared to others^{7,9,11} stems from the ability to represent the location of the center of high-pressure systems, and therefore to see the regional differences in wind speed and irradiance at kilometer-scale resolution. For example, the two extreme weather patterns Ww and HNFa have a high-pressure system located over Eastern Europe and Scandinavia-Iceland. These two patterns yield European mean anomalies in PV and wind power production of opposite signs. Due to the high impacts of atmospheric blockings, accurately forecasting such events in terms of location and duration is a much-needed meteorological service for the renewable energy sector. Despite the importance, there are uncertainties in representing blockings in models for numerical weather predictions²⁷. Future climate projections suggest a reduction in frequency and duration of atmospheric blockings compared to the past^{27,28}, but rare high-impact events might be possible²⁷. It implies that blockings are also an increasing risk for future power production when we consider the impacts of climate change. Additionally, temporal sequences of different weather patterns leading to extremes can be addressed in future studies.

Our study indicates that synoptic weather patterns can be used to estimate the anomalies in PV and wind power production across Europe. An earlier study suggests that it is useful to forecast weather patterns with a focus on a daily time scale for wind power anomalies and a monthly time scale for PV power anomalies²⁹. Our results indicate that the monitoring of weather patterns associated with anomalies in both PV and wind power production can be useful across weather time scales, i.e., hours up to ten days. Such information is helpful for electricity system operators to replenish energy storage to balance an upcoming weather-induced shortage in power production. Weather pattern classifications like the one used here¹⁹ are already well established at meteorological services, e.g., it is monitored and reported by the German Weather Service. Using forecasts of weather patterns can therefore be a valuable meteorological service to quickly identify problematic weather conditions to inform stakeholders in energy system operation. This is possible without the need to routinely operate an energy system model and without the costly requirement to develop and implement a new warning index.

Methods

Modeling approach. The Renewable Energy Model (REM) simulates photovoltaic (PV) power, and both on- and offshore wind power production in Europe. Our simulation with REM uses 23 years of high-resolution meteorological data for 1995–2017 inclusively. The hourly meteorological data are taken from the COSMO-REA6 reanalysis dataset³⁰, namely 10-m wind speed, 2-m air temperature, and surface irradiance with a horizontal resolution of 6 km. COSMO-REA6 is a regional reanalysis dataset

based on the Consortium for Small-scale Modelling (COSMO, www.cosmo-model.org) model for numerical weather prediction. It has a horizontal resolution of 6 km and 40 vertical levels, with the initial and boundary conditions based on ERA-Interim reanalysis data³¹. Assimilated observational data include for instance radiosondes, wind profiler, aircraft, and station observations³⁰. This dataset was successfully used for renewable energy applications before for Europe and Germany^{14,32–37}. Note that the meteorological data has the same weather sequences as the data used in the weather pattern classification¹⁹ due to the assimilation of observations. In addition to the consistency with the weather patterns, our choice for using COSMO-REA6 is motivated by the proven skill for energy system assessments and the lack of a large ensemble of decadal predictions with a similarly high resolution for multiple European countries. COSMO-REA6 shows a negative bias of –1.4% in annual and spatial means of irradiance against satellite data but is one of the best gridded irradiance datasets currently available for this type of research³⁶. COSMO-REA6 is also known to reproduce characteristics of observed irradiance and wind speed in Germany³⁸ and often outperforms other observational products and reanalysis data in many metrics^{33,36,39}.

The combined process to produce the output for analyses is illustrated in Fig. 6a. To substantially speed up the simulation and retaining the meteorological accuracy of the original data, we calculate the power production in every eighth grid box, giving us information on the power production on a horizontal grid of 48 km but using the benefits of the 6 km resolution of the original meteorological input data at every grid point, following an earlier approach⁴. This choice is made to represent consistent meteorological developments in the power simulations free of artifacts that could be introduced through interpolation of the meteorological data to a coarser spatial resolution.

REM’s PV power component was documented earlier^{4,36}. The locations of the PV power plants were obtained from www.wiki-solar.org (as of 2019-03-04). The effective irradiance, i.e., the

irradiance received on the titled PV modules, is calculated from the direct and diffuse radiation fluxes using geometry and a model for transferring the diffuse irradiance from the horizontal to the plane of the array⁴⁰, as in previous studies^{4,36}. The optimal tilt angles were obtained by maximizing the PV power production based on irradiance data for 2014, resulting in tilt angles of 21° to 50° as we go from southern to northern Europe. An estimate of error derived from using one year of data (2014) compared to 20 years (1995–2014) for 10 stations in the Baseline Surface Radiation Network (BSRN) showed a maximum error of 0.35%⁴¹. The optimal tilt angles are multiplied by a factor of 0.7 to reduce the shadow effects as investors typically make for economic reasons⁴². The azimuth angles were assumed to face south for all PV arrays. REM uses the power-rating model for crystalline silicon modules⁴³. The conversion rate is an empirical function based on ambient temperature, wind speed at the panel, and irradiance⁴³. Methods for PV power calculations like the one in REM were shown to have a good accuracy at a smaller computational burden, compared to other methods of power production estimates⁴⁴.

The wind power component uses a cubic power curve for calculating the wind power potential, following the method in previous studies^{11,45}. The potential capacity factor, denoted *C*, is calculated as in Eq. (1).

$$C = \begin{cases} 0 & \text{if } v_{hub} < v_{cut-in} \\ \frac{v_{hub}^3 - v_{cut-in}^3}{v_{rated}^3 - v_{cut-in}^3} & \text{if } v_{cut-in} \leq v_{hub} < v_{rated} \\ 1 & \text{if } v_{rated} \leq v_{hub} < v_{cut-out} \\ 0 & \text{if } v_{cut-out} \leq v_{hub} \end{cases} \quad (1)$$

where v_{hub} is the wind speed at hub height. v_{cut-in} and $v_{cut-out}$ are cut-in and cut-out wind speeds, defined as the threshold wind speeds for the onset and stop of producing power with the wind turbine, v_{rated} is the wind speed where the power production

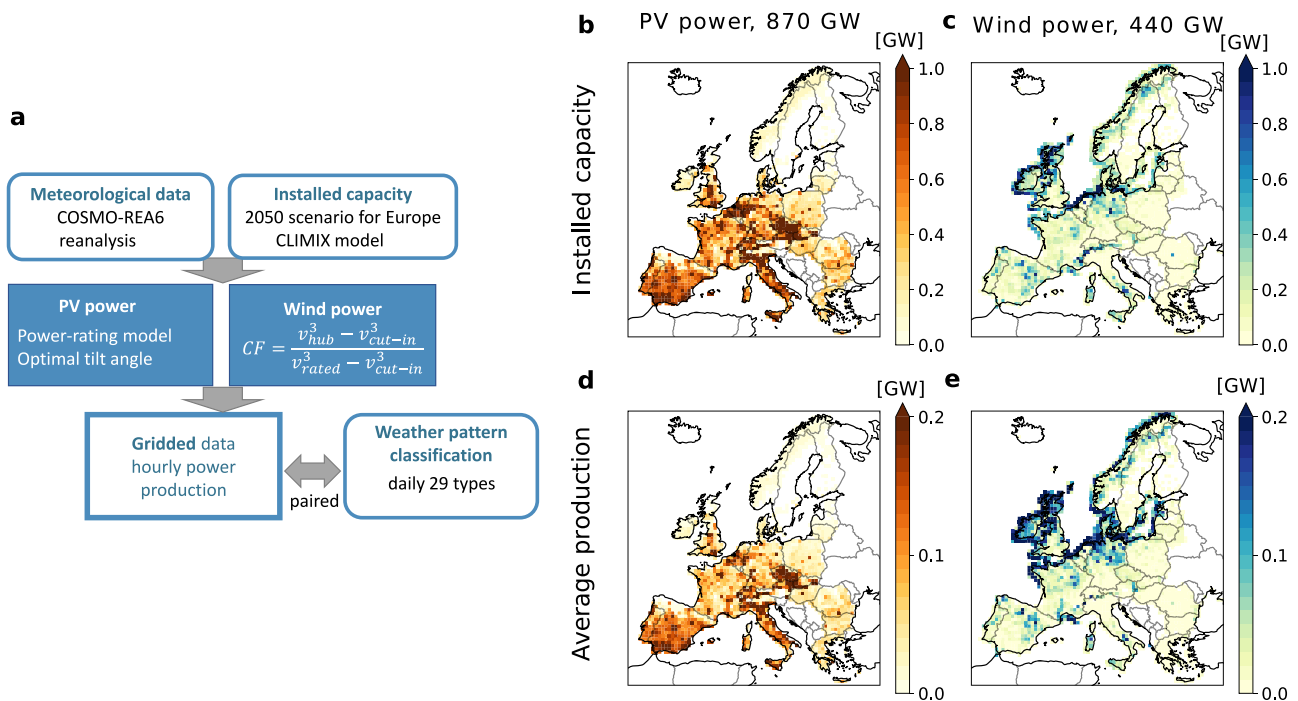


Fig. 6 Components of the Renewable Energy Model (REM). **a** Flow chart of REM used in this study. **b, c.** Installed capacity (GW) of PV and wind power in Europe in the scenario-2050 of the CLIMIX model¹⁵. **d, e.** Average hourly production (GW) of PV and wind power with the 2050 installation using weather of the period 1995–2017. All data is coarse-grained to a 48 km horizontal resolution, but is calculated using the original 6 km resolution such that the benefit of the high resolution for the meteorological data is retained.

reaches the maximum of production for which the turbine was designed, the so-called rated power.

REM simulates wind power production at a wind speed for v_{cut-in} v_{rated} $v_{cut-out}$ of 3.5, 13, 25 m s⁻¹ for all wind turbines, as in earlier wind power simulations^{4,15}. Turbine types have specific values for this wind power curve⁴⁶. We calculate v_{hub} from wind speeds at the two model levels 36 and 37 in COSMO-REA6 which corresponds to typical turbine hub heights from CLIMIX, e.g., 116 m and 178 m above mean sea level for mean meteorological conditions. Hub heights of the wind turbines in the CLIMIX model vary from 17 m to 150 m above ground level, but most are about 100 m above ground level and, therefore, fall within the layer between the chosen levels for a wind speed interpolation over land, and an extrapolation to some comparably few lower hub heights. Turbines in offshore regions are typically higher than on land, with values around 150 m in CLIMIX, and fall within the layer for interpolating the wind speeds from COSMO-REA6 output. Wind speed is the dominant driver of power differences, although air density also has an influence on the wind power output. In fact, the influence of variable air density on wind power production is two orders of magnitude smaller than the influence of wind on power production^{33,47}. For this reason and out of simplicity, REM uses a constant value of 1.2295 kg m⁻³ for air density in the wind power calculation, consistent with other studies^{4,45,47}.

We compare the REM output for the potentials of PV and wind power, i.e., calculated with irradiance and 100-m wind speed data. Data for validation are from the Climate Data Store (CDS)^{48,49} dataset Climate and energy indicators for Europe and from the website Renewables Ninja (www.renewables.ninja)^{50,51}. This is because the datasets for validation provide gridded data for potentials. The data for power production are provided at country-aggregated and with different installed capacities, and thus, not comparable. The REM output and the CDS data have different spatial resolutions and domain boundaries since they are based on different reanalysis datasets, namely COSMO-REA6³⁰, ERA5⁵², and MERRA-2⁵³. For this reason, we selected only grid cells inside four countries (Norway, Germany, Czech Republic, and Spain) to be comparable between the three datasets. For validation, we use potentials of PV and onshore wind power from REM. Wind power offshore was not calculated as country masks do not include the area of the offshore wind power plants. From CDS, we selected two variables: solar photovoltaic power generation and wind power generation onshore. From Renewables Ninja, we selected PV national current and Wind national current (Wind onshore current for Germany and Spain). We then spatially averaged these data to get their time series of potentials over the period 1995–2017. The temporal correlation coefficients between the hourly output of these datasets and our REM simulation with the scale-2019 installations for PV power range from 0.88 to 0.98 and for onshore wind power from 0.75 to 0.97, for the four selected countries shown in Supplementary Fig. S7. REM shows similar distributions of hourly PV and wind power production compared to the other datasets for the four countries and typically falls within the uncertainty in the distributions between CDS and Renewables Ninja. One noticeable difference is for PV power in Spain where REM simulates more high values compared to CDS and Renewables Ninja (Supplementary Fig. S7b). This is the benefit of the higher horizontal resolution of the meteorological data COSMO-REA6 in REM. It allows the simulation of clear and cloud-free skies in more grid cells which results in higher values of PV power production which is most noticeable in southern Europe with high irradiance. Comparing the average hourly potential, REM therefore also simulates larger average hourly potentials for PV power compared to CDS and Renewables Ninja (14%, 12%, and 13%, respectively). The average hourly potential for onshore wind power is comparable (24%,

23%, and 24%, respectively). Differences in the potentials between the datasets may arise from the different reanalysis data^{54,55}.

The model uses installed PV and wind power capacities projected for the year 2050 to account for the projected increase in renewable power plants that is expected for the coming years. The gridded data for the installed capacity for PV and wind power production stem from the 2050 scenario of the model on climate and energy mix (CLIMIX) with a horizontal resolution of 0.11°, approximately 12.5 km¹⁵ (Fig. 6b, c). CLIMIX integrates for instance information on the PV and wind power resource availability, forbidden locations (e.g., forest and sea for PV power and land for wind power offshore), and planned total installed capacities for the year 2050 from the 80% RES pathway for electricity production in the Roadmap 2050⁵⁶. Resource availability for PV and wind power in CLIMIX was determined based on surface irradiance and 10-m wind speed derived from a Weather Research and Forecast (WRF) model⁵⁷ simulation nudged to ERA-Interim³¹ reanalysis data for the period 2000–2012. CLIMIX does not explicitly consider hybrid plants but the grid cells typically contain both PV and wind power plants. The PV and wind power capacities do not change over time. Despite the static locations, CLIMIX data shows reasonable agreements between estimated power production and observed values for 2012¹⁵. Since the grid from CLIMIX (12.5 km) is finer than in REM (48 km), each REM grid cell contains several PV (wind) power plants from CLIMIX. The potential of an individual PV (wind) power plant was calculated and then multiplied by its corresponding installed capacity from CLIMIX to obtain its power production. Subsequently, the overall power production of one REM grid cell is the sum of the power production of all PV (wind) power plants inside that grid cell.

The installed capacities from CLIMIX are 870 GW for PV power and 440 GW for wind power, giving a ratio of PV-to-wind installed capacity of 2:1. The projected European total in onshore wind power is 259.8 GW and larger than the offshore capacity of 179.8 GW for 2050. Hub heights for onshore and offshore regions have a similar range but are in the mean larger offshore (121 m) than onshore (97.2 m). The total of PV and wind power capacities (1310 GW) is about 4.5 fold larger compared to the installed capacity in 2019 for Europe¹⁷, namely 287 GW including 120 GW of PV power and 167 GW of wind power installations resulting in a ratio of 0.7:1. The projected wind power in the CLIMIX model is conservative compared to, for example, another scenario for the European electricity in 2030 where the installed capacity of wind power is one-and-a-half times larger, namely 620 GW for wind power paired with 872 GW for PV power⁵⁸. Our choice of the CLIMIX model projection is motivated by the availability of gridded installations and the successful usage of the CLIMIX model to analyze the impacts of weather and climate change on renewable power in earlier studies^{11,21,59}.

With all the PV and wind power plants in the scenario-2050 installed capacities from CLIMIX (Fig. 6b, c), REM yields an average potential of 26% for wind power and 15% for PV power, which is comparable to other studies using installed capacities for 2015^{50,51}. The model yields a mean hourly production for Europe of 130 GW for PV power and 151 GW for wind power for the 2050 installed capacity, which gives a ratio of PV to PV plus wind power production of 46%. Our model captures regional differences in weather impacts accounting for the heterogeneous distribution of installed capacities. Some examples of regional clusters of high production are European cities with roof-top PV panels and offshore wind farms in the North Sea and around the British Isles (Fig. 6b, c).

Due to the lack of a comparable dataset of present-day installed capacity of PV and wind power, we simulate the present-day installed capacity (scale-2019) by scaling the gridded data for the

capacities of scenario-2050 such that they match the Europe-aggregated capacity for PV and wind power in 2019. The 2019 installed capacities aggregated over Europe are namely 120 GW of PV power and 167 GW of wind power¹⁷. The scaling approach decreases the installed capacity simultaneously across Europe at the same rate for individual energy sources, i.e., by about a factor of 0.14 (0.4) relative to the 2050 capacity for PV (wind) power, but retains the spatial distribution of installations of 2050. The regional capacity in scale-2019 thus does not necessarily reflect the current regional installed capacity because countries increase their capacities at different speeds and their future locations are not always the same as today. For example, the installed capacities for wind power in scale-2019 for Germany, France, and Italy are smaller, larger, and roughly equal compared to the results from a study using the capacities in 2015⁷ (in the same order: 12.6, 14.2, and 7.6 GW, compared to 31.5, 9.0, and 7.9 GW). In the absence of present-day gridded data for installed capacities with a high spatial resolution across Europe, differences in scientifically estimated capacities are to be expected. For instance, past studies had differences in the installed capacity of wind power in 2015 for Germany, with 31.5 GW⁷ and 40 GW⁶. Our approach successfully reproduces the ratio of PV to PV plus wind power from a previous study⁶. For example, from scale-2019 for Germany, the ratio of PV to PV plus wind power for installed capacity is 49% and for yearly production is 29%, comparable to the results from a previous study with 49% and 32%, respectively⁶. We also find that the pattern of High pressure over Central Europe (HM) is associated with the lowest total production for Germany in our 2019 simulation in agreement with a study using installed capacities of 2015⁶ (Supplementary Fig. S1). We further compared the temporal variability in hourly production from REM's scale-2019 simulation against actual production data from the ENTSO-E Transparency Platform (transparency.entsoe.eu)⁶⁰ for the year 2017, which is the last year for the meteorological data from COSMO-REA6. One cannot expect a close agreement with ENTSO-E for the hourly amount of country-aggregated power production due to differences in the installations and in the meteorological data. Nevertheless, REM's output has a similar temporal variability in the hourly PV and wind power production compared to the ENTSO-E data for 2017, with Pearson correlation coefficients of 0.95–0.97 for PV power and 0.56–0.69 for onshore wind power.

Analysis strategy. All results for power production associated with the weather patterns are calculated at an hourly time scale (unit GW), the same as the original output of the energy model to maintain its high temporal resolution. One exception is the daily production in the assessment of extremes of different duration namely 1, 5, and 10 days, all expressed in TWh per day. We calculate PV and wind power production for all time steps with valid data. We consider anomalies in terms of power production and do not simulate electricity demand or transmission. However, over- and underproduction would theoretically correspond to an over- or undersupply, if all else was equal.

We assess anomalies in PV and wind power production associated with different weather patterns. To that end, we use 29 different synoptic weather patterns for Europe from a dataset provided by the German Weather Service¹⁹. Each day is associated with one particular weather pattern for the whole of Europe. The names of the weather patterns follow the official definition¹⁹. To be compatible with the hourly output from REM, we assign the same weather pattern of a given day to all 24 hours of the same day. To get Europe-aggregated hourly mean production classified by weather patterns, we calculate the hourly mean across all time steps associated with the same weather pattern. The 1995–2017 mean is then subtracted from this composite of mean production per

weather pattern to determine the anomaly in power production. For seasonal differences, semi-annual division for seasons is defined as in the classification of weather pattern¹⁹ for consistency, i.e., winter refers to 16 October to 15 April, and summer to 16 April to 15 October. Seasonal anomalies are calculated in a similar manner but by selecting time steps for winter and summer mean production.

For spatial differences, to calculate the power production anomalies for each weather pattern, gridded data with the time steps corresponding to that weather pattern are selected and hourly averaged to compile composite data for each weather pattern. Then the 1995–2017 mean power production or meteorological data for Europe is subtracted from the composite means per pattern (e.g., Figs. 4, 6d, e). Anomalies in power production associated with weather patterns are calculated in percentage relative to the mean production, i.e., subtracted and then divided by the mean for all-year or the season for the period 1995–2017 from the same simulation. Note that the different installed capacities for PV and wind power in the simulations imply different absolute power productions even when relative anomalies of individual energy sources are identical between the simulations.

Four regions, marked in Fig. 5, are chosen for an assessment of spatially averaged anomalies in power production considering different durations. The regions cover 20 x 20 grid boxes each and are selected for the following reasons. The northernmost part of Scandinavia (around 67.6°N, 20.1°E) is selected because of the contrast in the power production anomaly compared to Western Europe, e.g., Fig. 4b, c. Northern Germany paired with the North Sea (around 53.1°N, 7.0°E) is assessed due to the large number of installed wind power plants. The Iberia peninsula (around 39.9°N, 5.0°W) is investigated due to the high potential for PV power production. The Balkans and surrounding areas (40.3°N, 20.8°E) are analyzed due to the contrast in wind power production relative to Western Europe⁷.

To identify weather patterns associated with extremes in PV and wind power production of different durations, we first identify sets of consecutive days that have the same weather pattern for at least 1, 5, and 10 days, referred to as 1-, 5-, and 10-day events. One day is a typical time frame used in past studies and chosen here for the comparability to past results. Ten days is a typical time period for the limit of weather forecasting beyond which the predictability of the weather strongly declines. We additionally choose five days to assess one interim point in time. We obtained 8401, 443, and 19 events with 1-, 5- and 10-day duration, respectively. The year-to-year differences in the event occurrence can be large, e.g., zero to four events for 10-day events, but there is no perceptible strong long-term trends (see Supplementary Fig. S8). In each region, we compute the composite of 1-day means for the same weather pattern and subtract the 1-day mean for 1995–2017 to obtain the anomalies. The weather patterns associated with the lowest and highest power production are identified per duration and region (Fig. 5).

Data availability

COSMO-REA6 data is freely available at https://opendata.dwd.de/climate_environment/REA/COSMO_REA6/. The CLIMIX data was acquired from the author¹⁵. The output of REM and the source data for figures are available⁶¹ at https://www.wdc-climate.de/ui/entry?acronym=DKRZ_LTA_1198_ds00003.

Code availability

The code of REM and custom codes to reproduce the figures are available⁶¹ at https://www.wdc-climate.de/ui/entry?acronym=DKRZ_LTA_1198_ds00003.

Received: 23 February 2023; Accepted: 16 January 2024;

Published online: 01 February 2024

References

1. The European Commission. Stepping up Europe's 2030 climate ambition - Investing in a climate-neutral future for the benefit of our people. Communication from the commission to the European Parliament, the council, the European economic and social committee and the committee of the regions. <https://eur-lex.europa.eu/legal-content/EN/TXT/?uri=CELEX:52020DC0562> (2020).
2. European association for the cooperation of transmission system operators (TSOs) for electricity (ENTSO-E). ENTSO-E grid map 2015. <https://www.entsoe.eu/data/map/downloads/>. Accessed 24 Apr 2022.
3. Ten-Year Network Development Plan (TYNDP) 2022. Opportunities for a more efficient European power system in 2030 and 2040 <https://eepublicdownloads.blob.core.windows.net/public-cdn-container/tyndp-documents/TYNDP2022/public/system-needs-report.pdf> (2022). version for public consultation, Accessed: 15 Dec 2022.
4. Frank, C., Fiedler, S. & Crewell, S. Balancing potential of natural variability and extremes in photovoltaic and wind energy production for European countries. *Renew. Energy* **163**, 674–684 (2020).
5. Brayshaw, D. J., Troccoli, A., Fordham, R. & Methven, J. The impact of large scale atmospheric circulation patterns on wind power generation and its potential predictability: a case study over the UK. *Renew. Energy* **36**, 2087–2096 (2011).
6. Drücke, J. et al. Climatological analysis of solar and wind energy in Germany using the Grosswetterlagen classification. *Renew. Energy* **164**, 1254–66 (2020).
7. Grams, C. M., Beerli, R., Pfenninger, S., Staffell, I. & Wernli, H. Balancing Europe's wind-power output through spatial deployment informed by weather regimes. *Nat. Clim. Change* **7**, 557–562 (2017).
8. Couto, A., Costa, P., Rodrigues, L., Lopes, V. V. & Estanqueiro, A. Impact of weather regimes on the wind power ramp forecast in Portugal. *IEEE Trans. Sustain. Energy* **6**, 934–942 (2014).
9. van der Wiel, K. et al. The influence of weather regimes on European renewable energy production and demand. *Environ. Res. Lett.* **14**, 094010 (2019).
10. Bloomfield, H. C., Brayshaw, D. J. & Charlton-Perez, A. J. Characterizing the winter meteorological drivers of the European electricity system using targeted circulation types. *Meteorol. Appl.* **27** (2019).
11. van der Wiel, K. et al. Meteorological conditions leading to extreme low variable renewable energy production and extreme high energy shortfall. *Renew. Sustain. Energy Rev.* **111**, 261–275 (2019).
12. Michelangeli, P.-A., Vautard, R. & Legras, B. Weather regimes: recurrence and quasi stationarity. *J. Atmos. Sci.* **52**, 1237–1256 (1995).
13. Huang, W. T. K. et al. Weather regimes and patterns associated with temperature-related excess mortality in the UK: a pathway to sub-seasonal risk forecasting. *Environ. Res. Lett.* **15**, 124052 (2020).
14. EWI (Energiewirtschaftliches Institut an der Universität zu Köln). dena pilot study "Towards climate neutrality". Climate neutrality 2045—Transformation of final energy consumption and the energy system (2021). Published by the German Energy Agency GmbH (dena).
15. Jerez, S. et al. The CLIMIX model: a tool to create and evaluate spatially-resolved scenarios of photovoltaic and wind power development. *Renew. Sustain. Energy Rev.* **42**, 1–15 (2015).
16. Maimó-Far, A., Homar, V., Tantet, A. & Drobinski, P. The effect of spatial granularity on optimal renewable energy portfolios in an integrated climate-energy assessment model. *Sustain. Energy Technol. Assessments* **54**, 102827 (2022).
17. Audrey Errard, F. D.-A. & Goll, M. Electrical capacity for wind and solar photovoltaic power—statistics. https://ec.europa.eu/eurostat/statistics-explained/index.php?title=Electrical_capacity_for_wind_and_solar_photovoltaic_power_-_statistics#Increasing_capacity_for_wind_and_solar_over_the_last_decades (2021). Accessed: 2022-02-08.
18. Heide, D. et al. Seasonal optimal mix of wind and solar power in a future, highly renewable Europe. *Renew. Energy* **35**, 2483–2489 (2010).
19. James, P. An objective classification method for Hess and Brezowsky Grosswetterlagen over Europe. *Theor. Appl. Climatol.* **88**, 17–42 (2007).
20. Fiedler, S. et al. First forcing estimates from the future CMIP6 scenarios of anthropogenic aerosol optical properties and an associated Twomey effect. *Geosci. Model Dev.* **12**, 989–1007 (2019).
21. Jerez, S. et al. The impact of climate change on photovoltaic power generation in Europe. *Nat. Commun.* **6**, 1–8 (2015).
22. Zscheischler, J. et al. A typology of compound weather and climate events. *Nat. Rev. Earth Environ.* **1**, 333–347 (2020).
23. Zappa, W. & Van Den Broek, M. Analysing the potential of integrating wind and solar power in Europe using spatial optimisation under various scenarios. *Renew. Sustain. Energy Rev.* **94**, 1192–1216 (2018).
24. Sillmann, J. & Croci-Maspoli, M. Present and future atmospheric blocking and its impact on European mean and extreme climate. *Geophys. Res. Lett.* **36** (2009).
25. Gibson, P. B. & Cullen, N. J. Synoptic and sub-synoptic circulation effects on wind resource variability—a case study from a coastal terrain setting in New Zealand. *Renew. Energy* **78**, 253–263 (2015).
26. Ohba, M., Kadokura, S. & Nohara, D. Impacts of synoptic circulation patterns on wind power ramp events in East Japan. *Renew. Energy* **96**, 591–602 (2016).
27. Woollings, T. et al. Blocking and its response to climate change. *Curr. Clim. Change Rep.* **4**, 287–300 (2018).
28. Dorrington, J., Strommen, K., Fabiano, F. & Molteni, F. CMIP6 models trend toward less persistent European blocking regimes in a warming climate. *Geophys. Res. Lett.* **49**, (2022).
29. Bremen, L. V. Large-Scale Variability of Weather Dependent Renewable Energy Sources. In: *Management of Weather and Climate Risk in the Energy Industry*, (ed Troccoli, A.) 189–206 (Springer Netherlands, 2010).
30. Bollmeyer, C. et al. Towards a high-resolution regional reanalysis for the European CORDEX domain. *Q. J. Roy. Meteorol. Soc.* **141**, 1–15 (2015).
31. Dee, D. P. et al. The ERA-Interim reanalysis: Configuration and performance of the data assimilation system. *Q. J. Roy. Meteorol. Soc.* **137**, 553–597 (2011).
32. Frank, C. W. et al. Bias correction of a novel European reanalysis data set for solar energy applications. *Sol. Energy* **164**, 12–24 (2018).
33. Frank, C. W. et al. The added value of high resolution regional reanalyses for wind power applications. *Renew. Energy* **148**, 1094–1109 (2020).
34. Henckes, P., Knaut, A., Obermüller, F. & Frank, C. The benefit of long-term high resolution wind data for electricity system analysis. *Energy* **143**, 934–942 (2018).
35. Kaspar, F. et al. Regional atmospheric reanalysis activities at Deutscher Wetterdienst: review of evaluation results and application examples with a focus on renewable energy. *Adv. Sci. Res.* **17**, 115–128 (2020).
36. Kenny, D. & Fiedler, S. Which gridded irradiance data is best for modelling photovoltaic power production in Germany? *Sol. Energy* **232**, 444–458 (2022).
37. Weide Luiz, E. & Fiedler, S. Spatio-temporal observations of nocturnal low-level jets and impacts on wind power production. *Wind Energy Sci. Discussions* 1–28 (2022).
38. Camargo, L. R., Gruber, K. & Nitsch, F. Assessing variables of regional reanalysis data sets relevant for modelling small-scale renewable energy systems. *Renew. Energy* **133**, 1468–1478 (2019).
39. Borsche, M., Kaiser-Weiss, A. K. & Kaspar, F. Wind speed variability between 10 and 116 m height from the regional reanalysis COSMO-REA6 compared to wind mast measurements over Northern Germany and the Netherlands. *Adv. Sci. Res.* **13**, 151–161 (2016).
40. Klucher, T. M. Evaluation of models to predict insolation on tilted surfaces. *Sol. Energy* **23**, 111–114 (1979).
41. Frank, C. W. *The Potential of High Resolution Regional Reanalyses Cosmo-rea for Renewable Energy Applications*. Ph.D. thesis, University of Cologne, Germany (2019).
42. Saint-Drenan, Y.-M., Wald, L., Ranchin, T., Dubus, L. & Troccoli, A. An approach for the estimation of the aggregated photovoltaic power generated in several European countries from meteorological data. *Adv. Sci. Res.* **15**, 51–62 (2018).
43. Huld, T. et al. A power-rating model for crystalline silicon PV modules. *Sol. Energy Mater. Sol. Cells* **95**, 3359–3369 (2011).
44. Dittmann, S. et al. Results of the 3rd modelling round robin within the European project "PERFORMANCE"—comparison of module energy rating methods. Presented at the 25th European Photovoltaic Solar Energy Conference and Exhibition, 4333–4338 (Valencia, Spain 2010).
45. Henckes, P., Frank, C., Küchler, N., Peter, J. & Wagner, J. Uncertainty estimation of investment planning models under high shares of renewables using reanalysis data. *Energy* **208**, 118207 (2020).
46. Wang, Y., Hu, Q., Li, L., Foley, A. M. & Srinivasan, D. Approaches to wind power curve modeling: a review and discussion. *Renew. Sustain. Energy Reviews* **116**, 109422 (2019).
47. Tobin, I. et al. Assessing climate change impacts on European wind energy from ENSEMBLES high-resolution climate projections. *Clim. Change* **128**, 99–112 (2015).
48. Copernicus Climate Change Service. Climate and energy indicators for Europe from 1979 to present derived from reanalysis <https://cds.climate.copernicus.eu/cdsapp#!/dataset/sis-energy-derived-reanalysis?tab=form> (2020). Data retrieved from Climate Data Store (CDS), Accessed 3 June 2021.
49. Dubus, L. et al. C3S Energy: A climate service for the provision of power supply and demand indicators for Europe based on the ERA5 reanalysis and ENTSO-E data. *Meteorol. Appl.* **30**, e2145 (2023).
50. Staffell, I. & Pfenninger, S. Using bias-corrected reanalysis to simulate current and future wind power output. *Energy* **114**, 1224–1239 (2016).
51. Pfenninger, S. & Staffell, I. Long-term patterns of European PV output using 30 years of validated hourly reanalysis and satellite data. *Energy* **114**, 1251–1265 (2016).
52. Rohrer, M., Martius, O., Raible, C. & Brönnimann, S. Sensitivity of blocks and cyclones in ERA5 to spatial resolution and definition. *Geophys. Res. Lett.* **e2019GL085582** (2019).
53. Gelaro, R. et al. The modern-era retrospective analysis for research and applications, version 2 (MERRA-2). *J. Clim.* **30**, 5419–5454 (2017).
54. Urraca, R. et al. Evaluation of global horizontal irradiance estimates from ERA5 and COSMO-REA6 reanalyses using ground and satellite-based data. *Sol. Energy* **164**, 339–354 (2018).

55. Niermann, D., Borsche, M., Kaiser-Weiss, A. K. & Kaspar, F. Evaluating renewable-energy-relevant parameters of COSMO-REA6 by comparison with satellite data, station observations and other reanalyses. *Meteorologische Z.* **28**, 347–360 (2019).
56. European Climate Foundation. Roadmap 2050: a practical guide to a prosperous, low carbon Europe. *Brussels: ECF* (2010).
57. Skamarock, W. C. et al. A description of the advanced research WRF version 3. *NCAR Techn. Note* **475**, 113 (2008).
58. European Commission, Joint Research Centre (JRC). Global Energy and Climate Outlook 2020: Energy, Greenhouse gas and Air pollutant emissions balances. *Dataset* <https://data.jrc.ec.europa.eu/dataset/1750427d-afd9-4a10-8c54-440e764499e4> (2020). Accessed 24 Apr 2022.
59. Tobin, I. et al. Climate change impacts on the power generation potential of a European mid-century wind farms scenario. *Environ. Res. Lett.* **11**, 034013 (2016).
60. Hirth, L., Mühlenpfordt, J. & Bulkeley, M. The ENTSO-E transparency platform—a review of Europe’s most ambitious electricity data platform. *Appl. Energy* **225**, 1054–1067 (2018).
61. Ho, L., Fiedler, S. & Wahl, S. PV and Wind power dataset for Europe. https://www.wdc-climate.de/ui/entry?acronym=DKRZ_LTA_1198_ds00003 (2023).

Acknowledgements

This study has been conducted in the framework of the Hans-Ertel-Centre for Weather Research funded by the German Federal Ministry for Transportation and Digital Infrastructure (grant number BMVI/DWD 4818DWDP5A). We thank the German Weather Service for providing COSMO-REA6 data, P. James for the data for the weather patterns, C. Frank for the code for photovoltaic power simulations, and S. Jerez for the CLIMIX data.

Author contributions

L.H. designed and ran the model experiments, analyzed the results, and created the figures. S.F. conceived the concept and led the study. Both authors wrote and reviewed the manuscript.

Funding

Open Access funding enabled and organized by Projekt DEAL.

Competing interests

The authors declare no competing interests.

Additional information

Supplementary information The online version contains supplementary material available at <https://doi.org/10.1038/s43247-024-01224-x>.

Correspondence and requests for materials should be addressed to Linh Ho-Tran.

Peer review information *Communications Earth & Environment* thanks Linyue Gao and Merlinde Kay for their contribution to the peer review of this work. Primary Handling Editors: Ana Teresa Lima, Clare Davis and Martina Grecequet. A peer review file is available.

Reprints and permission information is available at <http://www.nature.com/reprints>

Publisher’s note Springer Nature remains neutral with regard to jurisdictional claims in published maps and institutional affiliations.



Open Access This article is licensed under a Creative Commons Attribution 4.0 International License, which permits use, sharing, adaptation, distribution and reproduction in any medium or format, as long as you give appropriate credit to the original author(s) and the source, provide a link to the Creative Commons license, and indicate if changes were made. The images or other third party material in this article are included in the article’s Creative Commons license, unless indicated otherwise in a credit line to the material. If material is not included in the article’s Creative Commons license and your intended use is not permitted by statutory regulation or exceeds the permitted use, you will need to obtain permission directly from the copyright holder. To view a copy of this license, visit <http://creativecommons.org/licenses/by/4.0/>.

© The Author(s) 2024